Food Chemistry 159 (2014) 333–342

Contents lists available at ScienceDirect

Food Chemistry

journal homepage: www.elsevier.com/locate/foodchem

Cationic β-lactoglobulin nanoparticles as a bioavailability enhancer: Comparison between ethylenediamine and polyethyleneimine as cationizers

Zi Teng [a], Ying Li [a], Yuge Niu [b], Yuhong Xu [c], Liangli Yu [a,b], Qin Wang [a,*]

[a] Department of Nutrition and Food Science, University of Maryland, 0112 Skinner Building, College Park, MD 20742, United States
[b] Institute of Food and Nutraceutical Science, School of Agriculture and Biology, Shanghai Jiao Tong University, Shanghai 200240, China
[c] School of Pharmacy, Shanghai Jiao Tong University, Shanghai 200240, China

ARTICLE INFO

Article history:
Received 30 November 2013
Received in revised form 31 January 2014
Accepted 4 March 2014
Available online 14 March 2014

Keywords:
Cationic beta-lactoglobulin (CBLG)
Ethylenediamine (EDA)
Polyethyleneimine (PEI)
Nanoparticles
Mucoadhesive properties
Secondary structure
Protein digestion

ABSTRACT

Cationic β-lactoglobulin (CBLG) was synthesized by two strategies: extensive conjugation of ethylenediamine (EDA) and limited cationization with polyethyleneimine (PEI). Both methods provided CBLG with satisfactory water solubility and resistance to peptic digestion. Compared with EDA-derived CBLG (C-EDA), PEI-derived CBLG (C-PEI) exhibited a higher zeta potential (54.2 compared to 32.4 mV for C-EDA), which resulted in significantly elevated mucoadhesion (439% and 118% higher than BLG and C-EDA, respectively) in a quartz crystal microbalance (QCM) study. In addition, PEI caused reduced conformational disruption on BLG compared to EDA as evidenced by FTIR measurement. This character, together with the steric hindrance provided by PEI, caused a phenomenal reduction in tryptic digestibility by at least 75% compared to C-EDA. In the presence of aqueous acetone, C-PEI aggregated spontaneously into nanoparticles with average size of 140 nm and narrow size distribution. These merits made C-PEI a useful material that provides desirable solubility and protection for orally administrated nutraceuticals or drugs.

1. Introduction

In the past decades, nano-scaled encapsulation and delivery systems have attracted increasing attention as transporters for nutraceuticals or drugs (Augustin & Hemar, 2009; Jahanshahi & Babaei, 2008). Numerous nanoencapsulation strategies and systems have been developed by now, providing target compounds with desirable solubility (Luo & Wang, 2013), satisfactory stability (Guzey & McClements, 2006), controlled release properties (Teng, Luo, & Wang, 2013) and elevated bioavailability (Luo, Teng, Wang, & Wang, 2013). It is generally believed that the success of delivery is highly dependent on the surface properties of the encapsulant, such as charge and hydrophobicity (Futami, Kitazoe, Murata, & Yamada, 2007). Cationic polymers such as chitosan (Agnihotri, Mallikarjuna, & Aminabhavi, 2004), polylysine (Mislick, Baldeschwieler, Kayyem, & Meade, 1995) and lactoferrin (Bengoechea, Jones, Guerrero, & McClements, 2011), have demonstrated significantly higher mucoadhesive capacity and cellular internalization compared with anionic macromolecules. This phenomenon was largely attributed to two factors. The first factor is the affinity of the polycations to the negatively charged glycoproteins, the latter of which are abundant on the membrane of epithelia cells or tissues (e.g., small intestine wall) (Blau, Jubeh, Haupt, & Rubinstein, 2000). The second advantage for cationic encapsulants is their ability to acquire a negatively charged "corona" consisting mostly of serum proteins, which bind strongly to specific receptors on the cell membrane and thus promote the cellular internalization (Wang et al., 2013).

A wide array of cationic polymers have been exploited as novel encapsulating systems (Agnihotri et al., 2004; Bengoechea et al., 2011; Qi et al., 2012). However, these polymers are either insoluble at neutral pH (e.g., chitosan) or susceptible to digestion by pepsin or trypsin (e.g., polylysine). Therefore, the protection provided by these materials would be easily diminished when they enter the

Abbreviations: BLG, beta-lactoglobulin; CBLG, cationic BLG; PEI, polyethyleneimine; EDA, ethylenediamine dihydrochloride; C-EDA, EDA-derived CBLG; C-P600 and C-P1200, CBLG synthesized with PEI-600 and PEI-1200; EDC, *N*-(3-dimethylaminopropyl)-*N*-ethylcarbodiimide; PSM, porcine stomach mucin; TCA, trichloroacetic acid; PBS, phosphate buffer saline; QCM, quartz crystal microbalance; MALDI-TOF, matrix assisted laser desorption/ionization time-of-flight mass spectrometry; SEM, scanning electron microscopy; FT-IR, Fourier transform infrared spectroscopy; FSD, Fourier self deconvolution.

* Corresponding author. Tel.: +1 (301) 405 8421; fax: +1 (301) 314 3313.
E-mail address: wangqin@umd.edu (Q. Wang).

http://dx.doi.org/10.1016/j.foodchem.2014.03.022
0308-8146/

gastrointestinal tract, which is one of their major drawbacks. β-lactoglobulin (BLG), a 162-residue globulin, makes up approximately 60% of bovine whey protein (Kontopidis, Holt, & Sawyer, 2004). BLG is highlighted for its high surface charge and abundance of rigid β-sheet secondary structures. The first characteristic ensures the dispersion stability of BLG-based encapsulating systems even near its isoelectric point (~pH 5.0). The second property endows BLG with remarkable resistance against peptic digestion (Ko & Gunasekaran, 2006), thus providing maximal stability and controlled release for orally administrated bioactives.

To take advantage of both BLG and cationic polymers, our lab synthesized cationic BLG (CBLG) by grafting ethylenediamine (EDA) to the glutamic acid (Glu) or aspartic acid (Asp) residues of BLG (Teng, Li, Luo, Zhang, & Wang, 2013). The products exhibited highly positive surface charge, resulting in significantly improved mucoadhesion. In addition, they inherited the resistance to pepsin from BLG, whilst the digestion by trypsin was significantly promoted. A possible explanation for this phenomenon is the formation of Glu-/Asp-EDA conjugates (Teng, Li, Luo, Zhang, & Wang, 2013), which showed similar geometry and electric charge status to lysine. Since lysine is a known substrate for trypsin (Mattarella & Richardson, 1983), generation of Glu-/Asp-EDA conjugates might result in a significant increase in tryptic digestibility. Although increased tryptic digestibility provided EDA-derived CBLG with a certain degree of controlled release property, such change was unfavourable for delivering bioactive compounds that require prolonged protection after leaving the digestive tract and entering the circulatory system. Furthermore, the disintegration of EDA-derived CBLG implied the inability to gain the serum protein corona during circulation (Wang et al., 2013). This could not only compromise the efficacy of cellular uptake, but also lead to considerable cytotoxicity, since the corona plays a crucial role in counterbalancing the toxicity of cationic polymers (Lundqvist, 2013). Increased digestibility of CBLG, therefore, might be detrimental for its function as a bioavailability enhancer for certain nutraceuticals or drugs.

Polyethyleneimine (PEI, structure shown in Supplementary Fig. S1) is a cationic polymer whose repeating units consist of an amine and two methylene groups (–NH–CH_2–CH_2–). Owing to its low toxicity (Benjaminsen, Mattebjerg, Henriksen, Moghimi, & Andresen, 2012; Wiegand, Bauer, Hipler, & Fischer, 2013), PEI is permitted by the FDA to be added as an enzyme immobilizing agent in the beer industry (Carpenter, 1996). Amongst all PEI categories, branched PEI contains abundant primary amino groups that are reactive for cationization. Because of the high density of charge (one unit of positive charge in a mass unit of 43), conjugation of only a few PEI molecules is sufficient to introduce a significant amount of positive charges to the protein, without greatly altering its conformation (Futami et al., 2005). By far, PEI has been used for cationizing various proteins (Futami et al., 2007), resulting in significantly improved cellular uptake and low cytotoxicity.

Hereby, we propose the synthesis of CBLG using branched PEI as a cationizer. The anticipated structures of EDA-derived CBLG (C-EDA) and PEI-derived CBLG (C-PEI) are illustrated in Fig. 1. We hypothesised that C-PEI would exhibit similar resistance against pepsin, with superior mucoadhesion compared to BLG or C-EDA. Meanwhile, the product was expected to maintain its integrity under simulated intestinal conditions, because of the absence of Asp-/Glu-EDA conjugate, as well as steric hindrance provided by the PEI backbone. The product was compared in parallel with BLG and C-EDA, with respect to its conjugation degree, surface charge, secondary structure, *in vitro* digestibility and mucoadhesion. Finally, C-PEI-based nanoparticles were fabricated by organic solvent desolvation method, and the unique particle forming behaviours of C-PEI were reported.

2. Materials and methods

2.1. Materials

The following chemicals were purchased from Sigma–Aldrich (St. Louis, MO, USA): bovine BLG (90% purity), ethylenediamine dihydrochloride (EDA, 98% purity), branched polyethyleneimine (PEI600 and PEI1200, with average MW of 600 and 1200 Da, respectively), *N*-(3-dimethylaminopropyl)-*N*-ethylcarbodiimide (EDC, 97% purity), sinapinic acid, pepsin (3200–4500 units/mg), trypsin (10,000 BAEE units/mg), and trichloroacetic acid (TCA). Porcine stomach mucin (PSM, type III, containing 0.5–1.5% sialic acid) was obtained from Himedia Co., India. All other reagents (trifluoroacetic acid, simulated digestive fluids, etc.) were of analytical grade.

2.2. Preparation of cationic beta-lactoglobulin (CBLG)

CBLG was prepared by grafting cationic EDA or PEI moieties to the anionic carboxyl groups on the Asp and Glu residues of native BLG (Teng, Li, Luo, Zhang, & Wang, 2013). This was achieved via a previously reported EDC-aided reaction (Lu et al., 2005). BLG and the cationizers (EDA or PEI) were dissolved in deionized water at 20 and 100 mg/ml, respectively. The pH was then adjusted to 4.75 using 1 M HCl for BLG solution or concentrated HCl for cationizer dispersions. Thereafter, 5 ml of BLG solution was added slowly to 30 ml cationizer dispersion under mild stirring, and the mixture was incubated at room temperature for 15 min. Cationization was initiated by the addition of 30 mg EDC and terminated by adding 108 μl sodium acetate buffer (4 M, pH 4.75) after 4 h. The resultant dispersion was subjected to dialysis centrifugation (5000*g*, 30 min), using a Macrosep® centrifuge tube (Pall Corp., Ann Harbor, MI) with a built-in filtering membrane. Tubes with different MW cutoff values (10,000 for EDA and PEI-600-derived CBLG and 100,000 for PEI-1200-derived CBLG) were chosen for different samples in order to maximise the removal of unreacted chemicals, without compromising protein yield significantly. The retentate obtained after centrifugation was further dialyzed against deionized water at 4 °C for at least 48 h and freeze dried. The moisture content (Labuza, Tannenbaum, & Kerel, 1970) of the final product was less than 5%, and the protein content was above 90% according to a Bradford assay calibrated with BSA. The samples were designated as C-EDA for EDA-derived CBLG and C-P600/C-P1200 for CBLG synthesized with PEI-600/PEI-1200.

2.3. Determination of molecular weight and net charge

The molecular weights (MW) of BLG and CBLG were determined by matrix assisted laser desorption/ionization time-of-flight (MALDI-TOF) mass spectrometry in linear mode (Dai, Whittal, & Li, 1999). The samples were dispersed at 25 mg/ml in deionized water, which contained 1 μl/ml trifluoroacetic acid (TFA). The matrix solution was prepared by dissolving 10 mg sinapinic acid in a mixture of 200 μl pure acetonitrile and 200 μl water (containing 0.2 μl TFA). Prior to analysis, 1 μl matrix solution was spotted onto the target plate, and 1 μl of the sample solution was doped above the matrix layer. A second matrix layer (0.5 μl) was then dripped on top of the aforementioned two layers. Each layer was air dried at room temperature before doping the next one. The target plate was then loaded into a Shimadzu Axima-CFR MALDI-TOF spectrometer (Shimadzu North America, Columbia, MD, USA). Spectra were obtained by illuminating the samples with a N_2 laser beam (130 mJ per shot, 2 shots per second) and analysed with the Kompact software. For each sample, at least 150 spot spectra were

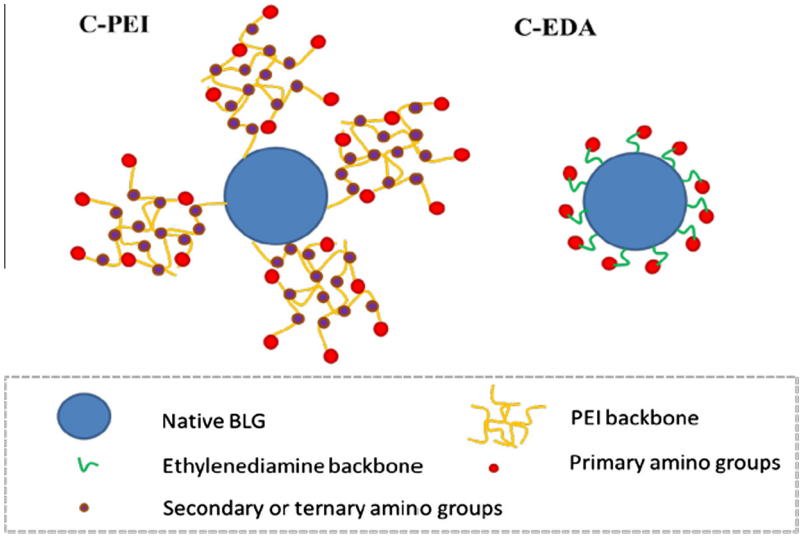

Fig. 1. Schematic illustration on the structure of PEI- and EDA-derived CBLG. The conjugates between EDA and Glu/Asp residues exhibit similar geometry and electric charge with lysine, a substrate for trypsin.

collected and averaged, and the peak values on the spectra were reported as the MW.

The amount of electric charge on CBLG was estimated based on the MW. The change in MW upon cationization (ΔM) was firstly converted to the conjugation degree (CD, number of EDA or PEI molecules grafted to a single BLG molecule), using the equation $CD = \Delta M/m$, where m represented the theoretical mass change when one cationizer was attached. The value of m was 42 for EDA, which was calculated by subtracting its MW (60) by the MW of water (18). For PEI-600 and PEI-1200, the values of m were estimated as 582 and 1182, respectively. The net charge was then calculated as follows: net charge = $z \times CD - 7$, where the number "−7" was the net charge of BLG molecules, CD was the conjugation degree, and z was the amount of positive charge on the cationizer. For EDA, the value of z was 2. For PEI, the z value was estimated as (molecular weight +26)/43 (Futami et al., 2005).

2.4. Determination of zeta potential

Samples were dispersed in PBS (10 mM, pH 7.0, same hereinafter) and measured for their electrophoretic mobility by laser Doppler velocimetry, using a Nano ZS90 Zetasizer (Malvern Inc., Malvern, UK). Each sample (1 mg/ml) was measured for three times, each time containing at least twelve runs. The data were then converted to zeta potentials using the Smoluchowski model.

2.5. Secondary structure determination

The structural change of BLG upon cationization was investigated by Fourier-transform infrared (FT-IR) analysis. Samples (3–5 mg) were freeze dried and mounted directly onto a Jasco FT/IR 4100 spectrometer (Jasco Inc., Easton, MD, USA). The infrared transmittance was recorded at wavenumbers between 1000 and 4000 cm^{-1} with resolution of 2 cm^{-1}. At least 100 repeated scans were undertaken for each sample. The spectra were averaged, smoothed, corrected for their baselines and converted to absorbance using the Spectra Manager software (Jasco Inc., Easton, MD, USA). For quantitative study on protein conformation, Fourier self-deconvolution (FSD) was undertaken on the obtained IR spectra, using the OMNIC software (Thermo Scientific, West Palm Beach, FL, USA). Peak finding and assignment were performed according to our previous study (Teng, Li, Luo, Zhang, & Wang, 2013).

2.6. Determination of in vitro digestibility

Samples were subjected to *in vitro* digestion test using two enzymes, i.e., pepsin and trypsin, following a procedure described in our previous study (Teng, Li, Luo, Zhang, & Wang, 2013). In brief, samples were dissolved in simulated gastric or intestinal fluid, incubated at 37 °C for 15 min, mixed with pepsin or trypsin solution at a substrate-to-enzyme ratio of 200:1 (w/w). At predetermined time intervals, aliquots of the sample were mixed with TCA solution to terminate digestion and then centrifuged. Digested protein was recovered in the supernatant and measured for its absorbance at 280 nm. For comparison purpose, another batch of samples (including BLG and CBLG) was digested by papain. The OD_{280} measured after peptic or tryptic digestion was divided by the one obtained from papain digestion, thus giving the relative digestibility for the samples.

2.7. Determination of mucoadhesion property

Quartz crystal microbalance (QCM) analysis (Wiecinski et al., 2009). QCM study was conducted as described in our previous study (Teng, Li, Luo, Zhang, & Wang, 2013). In brief, PSM dissolved in PBS was pumped through the sample chamber containing a gold-coated AT-cut quartz crystal, which had a fundamental frequency of 4.95 MHz (QSX-301, Q-Sense Co., Linthicum, MD, USA). The chamber was then rinsed by injecting pure PBS, after which BLG/CBLG dispersed in PBS was introduced. The deposition of PSM onto the quartz crystal and that of BLG/CBLG to the PSM layer induced two significant decreases in the frequency (Δf), which was recorded by QTools 3 software (Q-Sense Co., Linthicum, MD, USA). The Δf of the fifth overtone was converted to deposited mass (in ng/cm^2 crystal surface) by QTools 3, using the Sauerbrey model. Mucoadhesion was expressed as the mass ratio between deposited BLG/CBLG and PSM. The temperature of the chamber was kept at 37 °C during the measurement.

Turbidity analysis (Thongborisute & Takeuchi, 2008). Samples (BLG or CBLG) and PSM were dispersed in PBS at 10 and 1.2 mg/ml, respectively, and both passed through a 1.0 μm Acrodisc® syringe filter. The two stock solutions were then mixed at a proper

ratio and diluted appropriately to achieve a fixed PSM concentration of 1 mg/ml and different protein concentrations (0.25, 0.5 and 1.0 mg/ml). The mixture was then incubated at 37 °C for 1 h and cooled to room temperature. The absorbance at 400 nm of the mixture was recorded by a DU-730 UV/VIS spectrophotometer (Beckman Coulter Inc., Fullerton, CA, USA), using pure PSM dispersion (1 mg/ml, filtered as described above) as blank.

2.8. Preparation of BLG/CBLG nanoparticles

Nanoparticles were prepared with BLG/CBLG by desolvation (Teng, Luo, & Wang, 2012) method. Constant stirring (600 rpm) was applied throughout the particle formation process. The protein was dissolved in deionized water at 10 mg/ml (pH 7.5–8.0), and the resultant dispersion was equilibrated for 1 h at room temperature. To initiate particle formation, pure acetone was added dropwise to achieve an acetone/water ratio of 90/10 (v/v). The suspension changed from a clear solution into an opaque dispersion, which was equilibrated for 30 min. A crosslinker (glutaraldehyde) was then added to harden the particle structure. Based on the lysine content of BLG (16 mol Lys per mol BLG), the amount of glutaraldehyde needed for sufficient crosslinking is 40 μg/mg. After cationization, the content of primary amino groups in the protein increased significantly, and greater amount of glutaraldehyde was therefore required. In this study, the mass ratio between glutaraldehyde and protein ranged from 40 to 160 μg/mg. Prior to the crosslinking process, the dispersion was diluted with 90% (v/v) aqueous acetone by fivefold. The reason for dilution will be discussed in the Section 3.5. After 8 h of crosslinking, the suspension containing the nanoparticles was evaporated under nitrogen flow to remove acetone, supplemented with deionized water to the original volume (before dilution), and stored at 4 °C for subsequent assays.

2.9. Determination of particle size and count rate

The particle size and count rate of BLG/CBLG nanoparticle dispersions were determined (Teng, Luo, Wang, Zhang, & Wang, 2013) by dynamic laser scattering (DLS) using a BI-200 SM Goniometer Version 2 (Brookhaven Instrument Corp., Holtsville, New York, USA) equipped with a 35 mW He–Ne laser beam. The measurements were undertaken at two stages during the nanoparticle formation process: before dilution and after water supplementation. No further dilution was applied before the assays. The following parameters were adopted: laser power of 10 mW, detection wavelength of 637 nm, scattering angle of 90°, temperature of 25 °C, and measurement time of 1 min. The refractive indices and viscosities of different acetone/water systems were applied for all assays, since they were not significantly altered by low concentration of protein or glutaraldehyde in our study (data not shown). Two separate measurements were carried out on each sample in order to obtain accurate results. For count rate determination, the aperture pinhole size was fixed at 400 μm; to measure the particle size, appropriate aperture pinhole sizes were chosen to achieve a count rate between 100 and 300 kcps. The obtained data were analysed using cumulant algorithm, and the quadratic mean particle size was reported.

2.10. Scanning electron microscopy (SEM)

The morphology of BLG/CBLG nanoparticles was observed using a Hitachi SU-70 SEM (Hitachi, Pleasanton, CA, USA) (Teng et al., 2012). Approximately 40 μl of the nanoparticle dispersion was pipetted onto an aluminum pan and air dried. The pan was then cut into appropriate sizes and adhered to a 1-in. specimen stub with conductive carbon tapes (Electron Microscopy Sciences, Ft. Washington, PA, USA). Prior to observation, a thin layer (<20 nm) of gold and platinum was deposited to the samples using a sputter coater (Hummer XP, Anatech, CA, USA). Representative images are reported.

2.11. Statistics

All measurements were carried out in triplicate. The results are expressed as means ± standard error. Analysis of variance ($P < 0.05$) was performed on the data using SAS 9 software (SAS Institute Inc., Cary, NC, USA). The results were then subjected to Tukey's test with an experimentwise confidence level of $\alpha = 0.10$.

3. Results and discussion

3.1. Effect of cationization on net charge and zeta potential

Fig. 2 shows the mass/charge ratio (m/z) distribution of native and cationized BLG. BLG exhibited a major peak at $m/z = 18{,}215$ with a shoulder at $m/z = 18{,}314$. These values corresponded to mono-charged bovine BLG variants A and B, respectively (Chelulei Cheison, Brand, Leeb, & Kulozik, 2011; Dai et al., 1999). Meanwhile, doubly charged BLG molecules were also observed at $m/z = 9116$ (variant A) 9158 (variant B). Upon cationization, a significant shift towards higher values of m/z was observed. The peak for C-EDA centered at $m/z = 19{,}188$, indicating that approximately 21 EDA molecules were grafted to one BLG molecule. This result was in agreement with that obtained by TNBS assay (data not shown), which indicated that approximately 19 EDA molecules were conjugated on one BLG molecule. The reason why this number was higher than that achieved in our previous study (11 EDA per BLG molecule) was probably due to prolonged reaction time (Teng, Li, Luo, Zhang, & Wang, 2013). For PEI-derived CBLG, they exhibited a wider distribution of m/z values, probably because of the polydispersity of MW in commercially available PEI products as indicated by the manufacturer. The central m/z values for C-P600 and C-1200 were 21,305 and 23,231, respectively. As estimated from these results, an average of five PEI-600 and four PEI-1200 molecules were attached respectively to one BLG molecule.

Table 1 summarises the net charges and zeta potentials of BLG and CBLG. Native BLG, taking average of its two variants, possesses 16 Lys, 3 Arg, 10 Asp and 16 Glu residues (Chelulei Cheison et al., 2011), all of which results in an overall net charge of −7 per molecule. Upon cationization with EDA, the net charge of BLG shifted to +25. When PEI-600 and PEI-1200 were used as cationizers, the net charge shifted more dramatically to +58 (C-P600) and +102 (C-P1200), in spite of relatively low conjugation degrees. It should be pointed out, however, that the estimated net charge for PEI-derived CBLG was the maximal theoretical value that could only be achieved when all of the amino groups on PEI are protonated. The actual charging status of PEI-derived CBLG was highly dependent on the structure of PEI (e.g., chain length, degree of branching, content of primary and secondary amino groups), as well as the environment (pH, ionic strength, etc.) (Teng, Li, Luo, Zhang, & Wang, 2013).

Zeta potential reflects the surface charge and stability of colloidal particles. As shown in Table 1, native BLG exhibited a zeta potential of −35.8 mV, which was consistent with previous studies (Teng, Li, Luo, Zhang, & Wang, 2013). The zeta potential changed significantly to 32.4 mV upon conjugation with EDA, and it shifted towards more positive values for C-P600 (46.8 mV) and C-P1200 (53.4 mV). The high zeta potentials of PEI-derived CBLG were probably due to the abundance of amino groups on PEI. Moreover, a considerable part of these amino groups were pushed towards the surface of CBLG (Fig. 1), owing to the extended polymeric

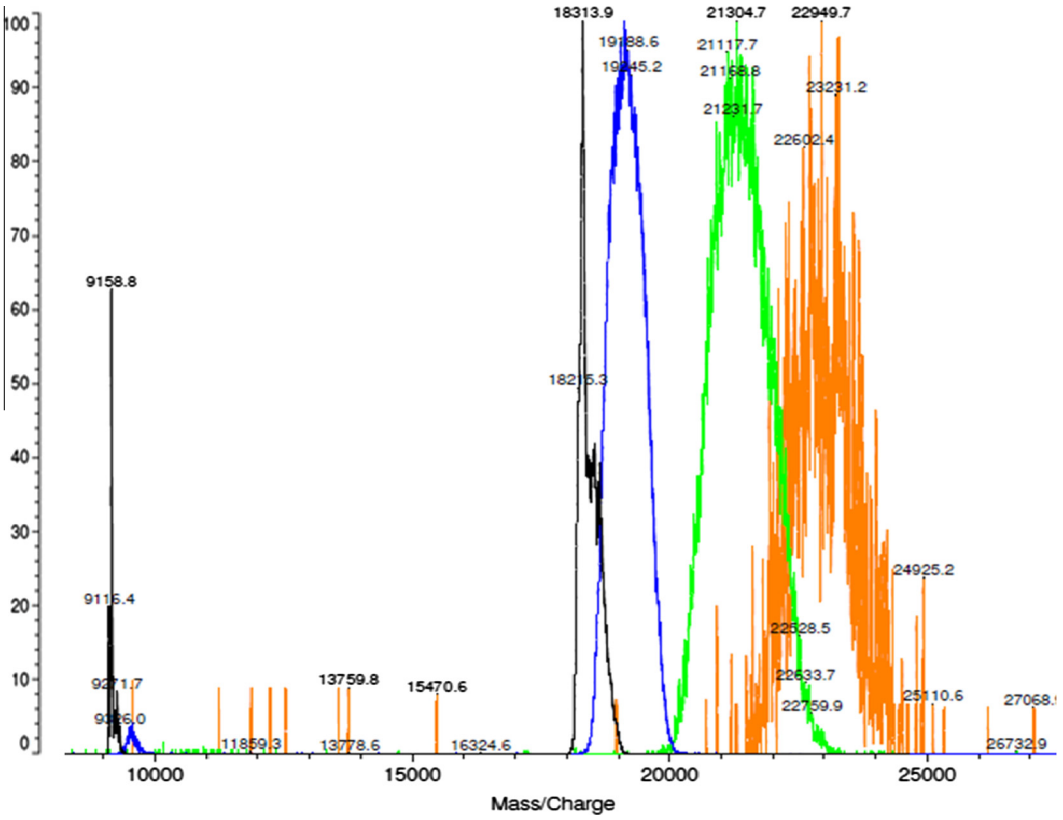

Fig. 2. MALDI-TOF spectra for BLG and CBLG.

Table 1
Conjugation degree and charging status of BLG and CBLG.

Sample name	Cationizer type	Peak MW (Da)	Conjugation degree*	Net charge per molecule*	Zeta potential in PBS (mV)**
BLG	–	18,215	–	−7	−35.8 ± 0.7[d]
C-EDA	EDA	19,188	20.8	+35	32.4 ± 1.0[c]
C-P600	PEI-600	21,305	5.2	+58	46.8 ± 1.5[b]
C-P1200	PEI-1200	23,231	4.2	+102	53.4 ± 1.3[a]

* The conjugation degrees were estimated from the peak MW measured by MALDI-TOF.
** Data with different letters showed significant difference (n = 3, $P<0.05$).

chains of PEI. This caused extensive exposure of protonated amino groups, which contributed to the highly positive zeta potential of C-PEI. As a result all CBLG samples were soluble in water or PBS at concentrations higher than 100 mg/ml, without any observable precipitation in several weeks (data not shown).

3.2. Change in protein structure upon cationization

The FT-IR spectra of BLG and different CBLG samples were displayed in Fig. 3. Native BLG exhibited three characteristic peaks: amide I (1631 cm^{-1}, C=O stretching), amide II (1520 cm^{-1}, C—N stretching and N—H bending), and amide III (1450 cm^{-1}, C—N stretching, N—H bending). The position of amide I (1631 cm^{-1}) was indicative for the predominance of β-sheet secondary structure in BLG, which was consistent with previous literatures (Kontopidis et al., 2004). After cationization with EDA, the amide I peak shifted to 1639 cm^{-1}, which suggested the formation of other secondary structures at the expense of the β-sheet. No other peak was observed with significant shifting. These phenomena could be explained by the fact that C=O stretching is more sensitive to conformational change than other common stretching or bending patterns in proteins (Dong et al., 1996). As protein molecules changed in their secondary structure, the intra-molecular hydrogen bonding was either strengthened or weakened, both of which altering the C=O pattern and leading to a shift in the amide I peak.

When PEI was used as a cationizer, the shift in amide I was not as significant as that for C-EDA. This phenomenon indicated a lesser extent of conformational change induced by PEI compared to EDA. This was possibly because only four to five Glu or Asp residues of BLG were substituted by PEI, whereas more than 20 EDA molecules were attached to BLG. As Glu and Asp are found mainly in the β-sheet region of BLG (Alexander et al., 1989), lower conjugation degree might be beneficial for the preservation of the original protein structure. On the other hand, amide II and amide III exhibited a significant shift towards higher wavenumbers. These changes were more likely attributed to the IR absorption of PEI sidechains rather than the change in protein conformation that they induced, considering the abundance of C—N and N—H bonding in PEI (Lakard, Herlem, Lakard, & Fahys, 2004). In addition, wide adsorption humps centered at 1075 and 1099 were observed for C-P600 and C-P1200, respectively. These peaks were assigned for C—N stretching of alkyl amines, which were typical for PEI (Khanam, Mikoryak, Draper, & Balkus, 2007).

For further investigation on secondary structure, the spectra were subjected to FSD and curve fitting. As shown in Table S1,

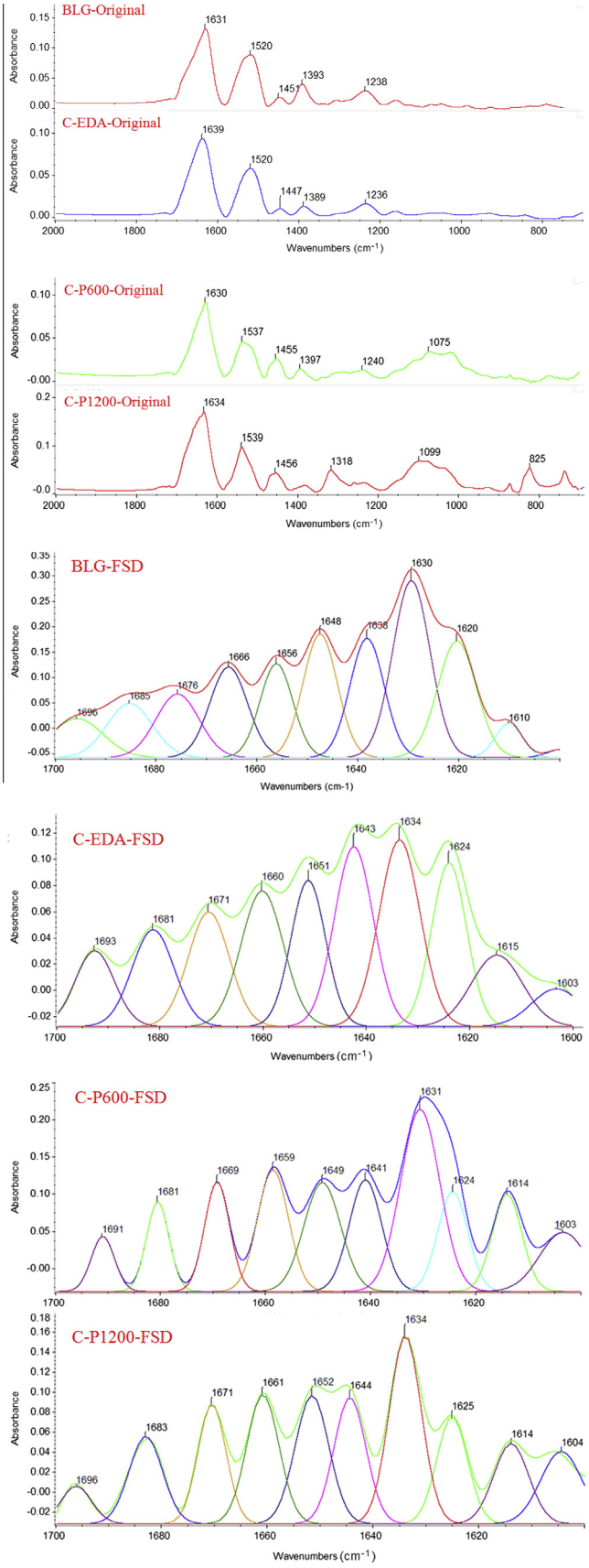

Fig. 3. Original and Fourier self-deconvoluted FT-IR spectra of BLG and CBLG.

native BLG contained 52.5% β-sheet. The predominance of β-sheet was considered responsible for the rigidity and indigestibility of BLG (Bhattacharjee et al., 2005). When BLG was cationized with EDA, there was a significant conversion of β-sheet (decreased by 29%) into α-helix (increased by 34%), turns (increased by 33%) and random coil (increased by 26%) (Dong et al., 1996). This change was attributed to the consumption of Asp and Glu, both of which are present in abundance in β-sheets (Alexander et al., 1989). Similar results were also observed on PEI-derived CBLG; however, the conformational change induced by PEI was not as significant as that cause by EDA. The content of β-sheet was decreased by 7% and 10% for C-P600 and C-P1200 respectively. As suggested by these data, conjugation of a smaller number (4 or 5) of bulky cationic molecules might have led to a lesser extent of conformational change, compared with the grafting of a greater number (more than 20) of small cations, although the former approach introduced a significantly greater amount of positive charge. In addition, the compositions of secondary structures for C-P600 and C-P1200 were not significantly different as shown in Table S1. This result suggested that, compared with the size of the cationizer, the structure (monomeric or polymeric) and number of cationic moieties might have played a more important role in determining the secondary structure of BLG. This postulation was further supported by a follow-up study (data not shown), in which cationization of BLG with PEI-1800 resulted in a similar extent of conformational change as PEI-600 and PEI-1200. Based on the discussions above, PEI might be a better reagent for cationizing BLG while preserving its unique structure. A similar hypothesis was also proposed in previous literatures (Futami et al., 2005).

3.3. In vitro digestibility of BLG and CBLG

The digestion profiles of BLG and CBLG are depicted in Fig. 4. Native BLG is highlighted for its resistance against peptic digestion. This characteristic was confirmed by our study, in which only 9% of BLG was digested by pepsin in SGF after 4 h. When BLG was cationized by EDA or PEI, its digestibility increased to 17% and 15%, respectively. This phenomenon was probably due to the disruption of β-sheet structure as discussed in the previous section. Such change might have led to higher flexibility of BLG molecules and increased exposure of their digestible sites, resulting in better accessibility of pepsin. Similar results were also reported and discussed in a previous literature (Mattarella & Richardson, 1983). In spite of the notable increase, the peptic digestibility of CBLG remained at a low level. Therefore, CBLG was expected to provide significant protection to incorporated nutraceuticals or drugs against digestion in the stomach.

Under simulated intestinal conditions, approximately 25% of BLG was digested by trypsin. A higher tryptic digestibility (32%) was observed for C-EDA, probably due to the formation of Asp-EDA/Glu-EDA conjugates (Teng, Li, Luo, Zhang, & Wang, 2013). As discussed before, such amino acid derivatives exhibited similar geometric structure and electronic charging status with lysine, a major substrate of trypsin. PEI, on the contrary, is a polymer with bulky branches and multiple positive charges, and the conjugate formed between Asp/Glu and PEI did not exhibit such similarity to lysine. In addition, the polymeric network of PEI might have acted as a barrier for trypsin (Fig. 1). As a result, the tryptic digestibility of C-P600 (8%) or C-P1200 (6%) was significantly lower than that of BLG or C-EDA. In addition, C-P600 and C-P1200 exhibited similar tryptic digestibility. Such phenomenon indicated that the structure (monomeric or polymeric, linear or branched) and number of conjugated cationic groups might be more important than

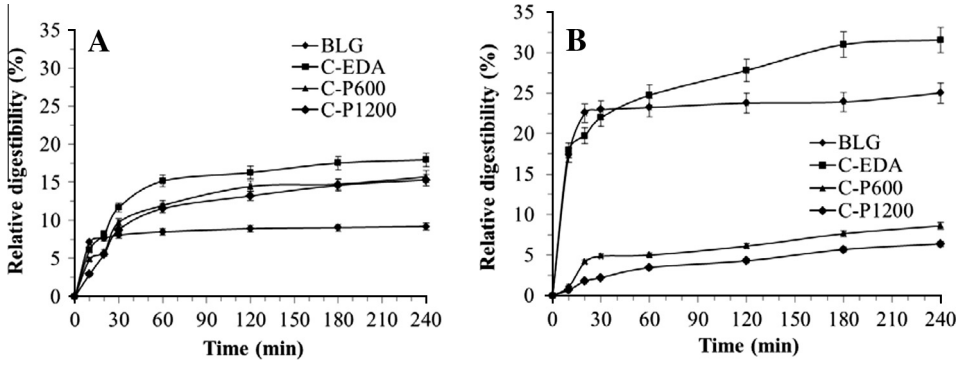

Fig. 4. *In vitro* peptic (A) and tryptic (B) digestion profiles of BLG and CBLG.

their size in determining the apparent digestibility of CBLG. This was similar with the findings in Section 3.2. Based on these results, PEI-derived CBLG may provide sufficient protection against both peptic and tryptic digestion, and such protection might remain effective after the target compound enters the circulatory system. This feature is favourable for the encapsulation and delivery of nutraceuticals and drugs that are susceptible to degradation or clearance by the circulatory system.

3.4. Mucoadhesive properties

Mucin is a highly glycosylated and negatively charged protein (Ludwig, 2005), which exists in abundance as a gel-like layer covering the small intestine wall. It serves as the first barrier for the entry of nutraceuticals or drugs into the circulatory system (Sogias, Williams, & Khutoryanskiy, 2008). Affinity to the mucin layer, known as mucoadhesion, is therefore a key factor that determines the bioavailability of orally administrated bioactives. In this study, two assays were performed to evaluate the mucoadhesion of BLG and CBLG. In the turbidity analysis (Fig. 5A), native BLG did not display any observable absorbance when mixed with mucin in PBS. However, CBLG exhibited significant absorbance at 400 nm, which suggested extensive formation of mucin-CBLG aggregates. In addition, the absorbance of C-P600 or C-P1200 was more than twice that of C-EDA. The electrostatic attraction between mucin and EDA/PEI moieties might have played a critical role in the aggregation process.

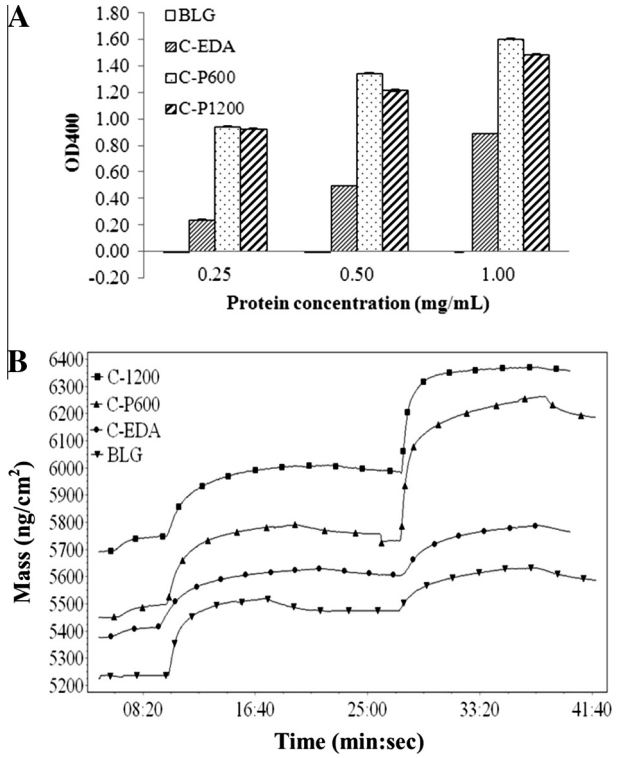

Fig. 5. Mucoadhesion of BLG and CBLG measured by (A) turbidity and (B) QCM-D.

The improvement in mucoadhesion by cationization was also evidenced by QCM. As shown in Fig. 5B, native BLG showed low affinity to the mucin layer that was pre-deposited onto the quartz crystal. After cationization, the mucoadhesion of BLG was increased significantly by 147%, 439%, and 366% for C-EDA, C-P600, and C-P1200, respectively (Table S2). Improved mucoadhesion was likely contributed by the high density of positive charge introduced with EDA or PEI. In addition, PEI-derived samples demonstrated more significant improvement in mucoadhesion than EDA, probably owing to its highly positive surface charge. The similarity in the mucoadhesive properties of C-P600 and C-P1200 was probably due to the similarity in their conformation as discussed before. In our preliminary study (data not shown), the surface hydrophobicity of C-P600 or C-P1200 was comparable to that of native BLG, which was significantly lower than that of C-EDA. Combining these results, we postulated that electrostatic attraction rather than hydrophobic interaction might have played a dominating role in the mucoadhesion process for CBLG. Based on the result on mucoadhesion and digestion, PEI-derived CBLGs might be a better solution for bioavailability enhancement for nutraceuticals or drugs.

It was worth mentioning that all studies on mucoadhesion were undertaken at neutral pH. Although some common cationic polymers (e.g., chitosan) were reported to be mucoadhesive (Modi, Joshi, & Sawant, 2013), these polymers were only positively charged at acidic pH, and they became insoluble at higher pH due to the deprotonation of their functional groups. The retention of positive charge over a wide range of physiologically relevant pHs is a major advantage of CBLG over other polycations, and such property makes CBLG an attractive vehicle for transporting bioactives through oral administration.

3.5. Nanoparticle forming behaviour of BLG and CBLG

The particle formation capabilities of BLG and CBLG are summarised in Table S3. In 90% acetone, native BLG formed particles with an average size of 136.3 nm. After crosslinking with glutaraldehyde and evaporation of acetone, the particles exhibited slightly increased size with decreased count rate. These results suggested that the majority of the particles maintained their size and structure (Teng et al., 2012). Similar results were observed for C-EDA,

which aggregated into smaller particles that kept virtually consistent size and count rate upon evaporation.

When PEI-derived CBLGs were used as particle formers, the results on particle sizes and count rates were similar to BLG and C-EDA. However, two major differences were observed. Firstly, the amount of glutaraldehyde needed for C-P600 and C-P1200 was at least 100% higher than that for BLG and C-EDA. Otherwise, the nanoparticles were prone to dissociation as indicated by a greatly decreased count rate of the dispersion (data not shown). This was probably because conjugation of PEI introduced a large amount of primary amino groups, which were the major substrate for glutaraldehyde-induced crosslinking (Weber, Coester, Kreuter, & Langer, 2000). As a result, a higher dose of glutaraldehyde was needed to achieve complete crosslinking. Furthermore, the positively charged amino groups introduced by PEI resulted in strong electrostatic repulsion between CBLG molecules. Such change necessitated more covalent bonds to overcome the repulsive force and maintain the compact structure of nanoparticles.

The second difference was that a dilution procedure was needed for the formation of nanoparticles, especially for C-P1200. In our preliminary study, C-P1200 formed a significant number of nanoparticles in 90% acetone, but these particles dissociated rapidly after evaporation. At lower glutaraldehyde doses (40–80 μg/mg protein), the nanoparticle dispersion became a clear solution after evaporation. When higher doses of glutaraldehyde (120–160 μg/mg protein) were applied, the dispersion turned into a dark-coloured gel. A possible explanation for these phenomena lay in the structure of branched PEI molecules. PEI possesses a highly branched structure with a large number of amino groups. However, only 30–40% of them are primary amino groups (Futami et al., 2007), which are reactive with glutaraldehyde. When PEI-derived CBLG formed nanoparticles, the surface of the particles was probably covered by PEI branches as indicated by the highly positive zeta potential. The distance between the two reactive amino groups, together with internal steric hindrance caused by the PEI network, could therefore impede glutaraldehyde molecules from effectively crosslinking within a single particle. On the other hand, due to the large number of nanoparticles in the dispersion, there was an increased chance for two nanoparticles to approach each other, expose their primary amino groups that could be connected by glutaraldehyde (Supplementary Fig. S2a). This could possibly explain the formation of gel instead of individual particles by C-P1200 after evaporation. When the dispersion was diluted, the chance for inter-particle crosslinking was greatly reduced, whereas the opportunity for crosslinking within a same particle was virtually unchanged (Supplementary Fig. S2b). Therefore, the average size and count rate of particles were better maintained. However, further studies need to be carried out to test this hypothesis and to establish new strategies to synthesize C-P1200-based nanoparticles.

Fig. 6 shows the morphology of nanoparticles formed by BLG (A), C-EDA (B) and C-P600 (C). The particles were approximately spherical and smooth at the surface. The sizes of BLG and C-EDA nanoparticles were slightly larger than that of C-P600 nanoparticles, which was consistent with the data from the DLS study. This difference was possibly caused by the repulsion between the bulky, highly charged PEI moieties on C-P600. The reason why sizes observed under SEM were generally lower than those obtained by DLS was probably the shrinkage of particles under vacuum (Luo, Teng, & Wang, 2012). Fig. 6(D) displays the structure of C-P600 nanoparticles after crosslinking and evaporation. Most of the particles maintained their original shape and size, although some large aggregates were observed under SEM.

3.6. Safety concerns for CBLG nanoparticles

Although CBLG possesses remarkable advantages, several safety issues related with this protein derivative need to be addressed

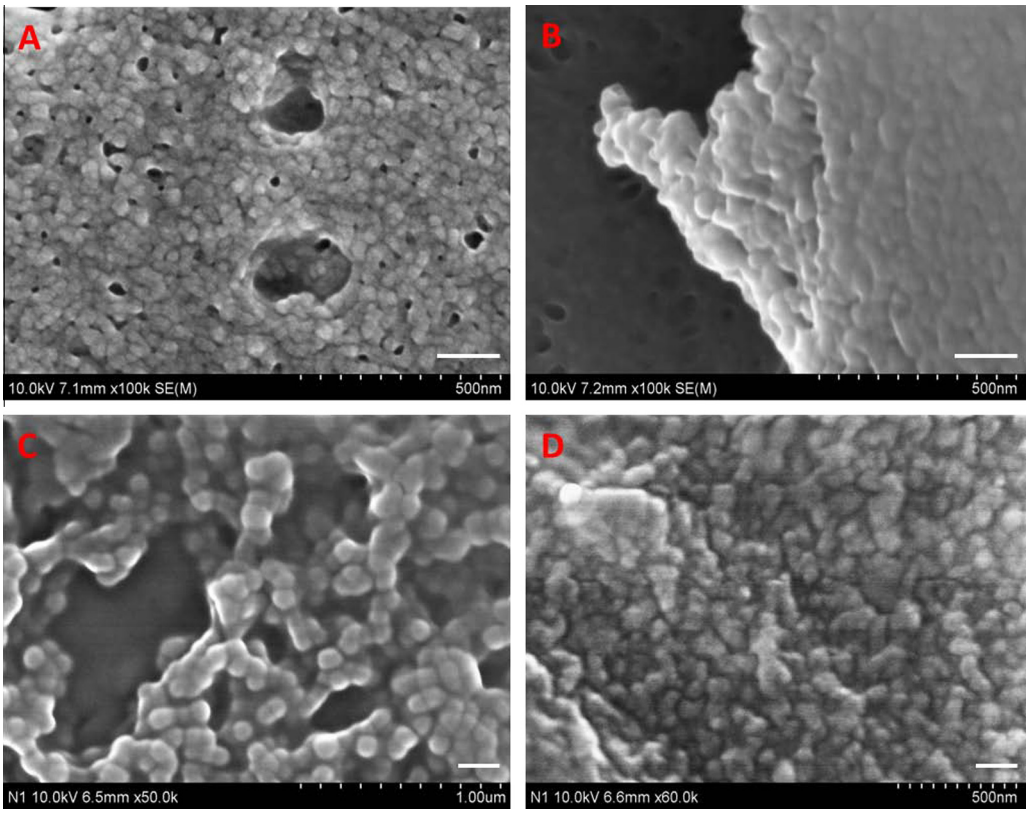

Fig. 6. SEM images of nanoparticles formed with (A) BLG, (B) EDA-derived CBLG, (C) PEI-derived CBLG, before evaporation, and (D) PEI-derived CBLG, after evaporation.

prior to its application in food industry. Polycations are known for significant cytotoxicity. However, PEI exhibits relatively low cytotoxicity compared to EDA, and thus it is permitted to be applied under certain circumstances in food industry (Carpenter, 1996). In addition, compared with pure PEI, PEI-BLG conjugates may exhibit much lower toxicity due to the low content of PEI moieties (4–5 PEI per CBLG molecule). Moreover, a recent study showed that the association between anionic serum protein and cationic polymer plays a vital role in mitigating the toxicity (Wang et al., 2013). Such protein–protein interaction would not compromise the cellular uptake of cationic nanoparticles; in fact, it was deemed as a chief contributor for elevated cellular internalization of these nano-scaled vehicles.

The existence of residual small molecules (EDC, glutaraldehyde and acetone) causes another concern for the safety of CBLG nanoparticles. However, unreacted chemicals and residual acetone could be maximally removed by common techniques such as dialysis or gel filtration. In addition, various chemicals including genipin and different enzymes are being developed as alternative crosslinkers (Dhayal, Gruppen, de Vries, & Wierenga, 2013). Substitution of glutaraldehyde by these food grade reagents would help reducing the toxicity significantly. However, further study needs to be conducted to determine the safe dose of CBLG nanoparticles.

4. Conclusions

CBLG was successfully synthesized from BLG using two strategies: coupling BLG with a larger quantity of cationic monomers (EDA) or with a smaller number of polycations (PEI-600 and PEI-1200). Both methods led to the reversal of net charge of BLG molecules, together with satisfactory dispersion stability at neutral pH. Compared with the EDA-involved approach, PEI-derived cationization resulted in a lower conjugation degree, but the net charge and zeta potential obtained from the latter approach was significantly higher than that achieved through the former one. Cationization with PEI led to less significant conformational change of BLG, resulting in better inheritance of the resistance against peptic digestion from native BLG. In addition, PEI-derived CBLG was more resistant against tryptic digestion than BLG as well as C-EDA. Substantial improvement in mucoadhesion was observed for PEI-derived CBLG compared to BLG or C-EDA, probably owing to the steric hindrance provided by PEI. Lastly, in the presence of acetone and glutaraldehyde, PEI-derived CBLG could aggregate into nanoparticles with an average size of 140 nm, and the formed particles maintained their morphology after evaporation (Supplementary Table S3). These characteristics made PEI-derived CBLG an attractive candidate as a bioavailability enhancer for poorly absorbed bioactives. Follow-up studies on the encapsulation property and releasing capacities as well as potential toxicity of CBLG nanoparticles are being conducted.

Acknowledgements

This research is partially supported by Maryland Agricultural and Experiment Station. The authors are grateful for the technical support of the Maryland NanoCenter of the University of Maryland in scanning electron microscopy.

Appendix A. Supplementary data

Supplementary data associated with this article can be found, in the online version, at http://dx.doi.org/10.1016/j.foodchem.2014.03.022.

References

Agnihotri, S. A., Mallikarjuna, N. N., & Aminabhavi, T. M. (2004). Recent advances on chitosan-based micro- and nanoparticles in drug delivery. *Journal of Controlled Release, 100*(1), 5–28.
Alexander, L. J., Hayes, G., Pearse, M. J., Beattie, C. W., Stewart, A. F., Willis, I. M., et al. (1989). Complete sequence of the bovine beta-lactoglobulin cDNA. *Nucleic Acids Research, 17*(16), 6739.
Augustin, M. A., & Hemar, Y. (2009). Nano- and micro-structured assemblies for encapsulation of food ingredients. *Chemical Society Reviews, 38*(4), 902–912.
Bengoechea, C., Jones, O. G., Guerrero, A., & McClements, D. J. (2011). Formation and characterization of lactoferrin/pectin electrostatic complexes: Impact of composition, pH and thermal treatment. *Food Hydrocolloids, 25*(5), 1227–1232.
Benjaminsen, R. V., Mattebjerg, M. A., Henriksen, J. R., Moghimi, S. M., & Andresen, T. L. (2012). The possible 'proton sponge' effect of polyethylenimine (PEI) does not include change in lysosomal pH. *Molecular Therapy, 21*(1), 149–157.
Bhattacharjee, C., Saha, S., Biswas, A., Kundu, M., Ghosh, L., & Das, K. P. (2005). Structural changes of beta-lactoglobulin during thermal unfolding and refolding-an FT-IR and circular dichroism study. *Protein Journal, 24*(1), 27–35.
Blau, S., Jubeh, T. T., Haupt, S. M., & Rubinstein, A. (2000). Drug targeting by surface cationization. *Critical Reviews in Therapeutic Drug Carrier Systems, 17*(5), 425–465.
Carpenter, W. T. (1996). Secondary direct food additives permitted in food for human consumption periodic acid and polyethylenimine. *Federal Register, 61*(28), 4871–4874.
Chelulei Cheison, S., Brand, J., Leeb, E., & Kulozik, U. (2011). Analysis of the effect of temperature changes combined with different alkaline pH on the β-lactoglobulin trypsin hydrolysis pattern using MALDI-TOF-MS/MS. *Journal of Agricultural and Food Chemistry, 59*(5), 1572–1581.
Dai, Y. Q., Whittal, R. M., & Li, L. (1999). Two-layer sample preparation: A method for MALDI-MS analysis of complex peptide and protein mixtures. *Analytical Chemistry, 71*(5), 1087–1091.
Dhayal, S. K., Gruppen, H., de Vries, R., & Wierenga, P. A. (2013). Controlled formation of protein nanoparticles by enzymatic cross-linking of α-lactalbumin with horseradish peroxidase. *Food Hydrocolloids, 36*, 53–59.
Dong, A., Matsuura, J., Allison, S. D., Chrisman, E., Manning, M. C., & Carpenter, J. F. (1996). Infrared and circular dichroism spectroscopic characterization of structural differences between beta-lactoglobulin A and B. *Biochemistry, 35*(5), 1450–1457.
Futami, J., Kitazoe, M., Maeda, T., Nukui, E., Sakaguchi, M., Kosaka, J., et al. (2005). Intracellular delivery of proteins into mammalian living cells by polyethylenimine-cationization. *Journal of Bioscience and Bioengineering, 99*(2), 95–103.
Futami, J., Kitazoe, M., Murata, H., & Yamada, H. (2007). Exploiting protein cationization techniques in future drug development. *Expert Opinion on Drug Discovery, 2*(2), 261–269.
Guzey, D., & McClements, D. J. (2006). Formation, stability and properties of multilayer emulsions for application in the food industry. *Advances in Colloid and Interface Science, 128–130*, 227–248.
Jahanshahi, M., & Babaei, Z. (2008). Protein nanoparticle: A unique system as drug delivery vehicles. *African Journal of Biotechnology, 7*(25), 4926–4934.
Khanam, N., Mikoryak, C., Draper, R. K., & Balkus, K. J. Jr., (2007). Electrospun linear polyethyleneimine scaffolds for cell growth. *Acta Biomaterialia, 3*(6), 1050–1059.
Ko, S., & Gunasekaran, S. (2006). Preparation of sub-100-nm beta-lactoglobulin (BLG) nanoparticles. *Journal of Microencapsulation, 23*(8), 887–898.
Kontopidis, G., Holt, C., & Sawyer, L. (2004). Invited review: β-Lactoglobulin: Binding properties, structure, and function. *Journal of Dairy Science, 87*(4), 785–796.
Labuza, T. P., Tannenbaum, S. R., & Kerel, M. (1970). Water content and stability of low-moisture & intermediate-moisture foods. *Food Technology, 24*(5), 35–36.
Lakard, S., Herlem, G., Lakard, B., & Fahys, B. (2004). Theoretical study of the vibrational spectra of polyethylenimine and polypropylenimine. *Journal of Molecular Structure: THEOCHEM, 685*(1), 83–87.
Lu, W., Zhang, Y., Tan, Y. Z., Hu, K. L., Jiang, X. G., & Fu, S. K. (2005). Cationic albumin-conjugated pegylated nanoparticles as novel drug carrier for brain delivery. *Journal of Controlled Release, 107*(3), 428–448.
Ludwig, A. (2005). The use of mucoadhesive polymers in ocular drug delivery. *Advanced Drug Delivery Reviews, 57*(11), 1595–1639.
Lundqvist, M. (2013). Nanoparticles: Tracking protein corona over time. *Nature Nanotechnology, 8*(10), 701–702.
Luo, Y., Teng, Z., & Wang, Q. (2012). Development of zein nanoparticles coated with carboxymethyl chitosan for encapsulation and controlled release of vitamin D3. *Journal of Agricultural and Food Chemistry*.
Luo, Y., Teng, Z., Wang, T. T. Y., & Wang, Q. (2013). Cellular uptake and transport of zein nanoparticles: Effects of sodium caseinate. *Journal of Agricultural and Food Chemistry, 61*(31), 7621–7629.
Luo, Y., & Wang, Q. (2013). Recent advances of chitosan and its derivatives for novel applications in food science. *Journal of Food Processing and Beverages, 1*(1), 1–13.
Mattarella, N. L., & Richardson, T. (1983). Physicochemical and functional properties of positively charged derivatives of bovine β-lactoglobulin. *Journal of Agricultural and Food Chemistry, 31*(5), 972–978.
Mislick, K. A., Baldeschwieler, J. D., Kayyem, J. F., & Meade, T. J. (1995). Transfection of Folate-Polylysine DNA complexes – Evidence for lysosomal delivery. *Bioconjugate Chemistry, 6*(5), 512–515.

Modi, J., Joshi, G., & Sawant, K. (2013). Chitosan based mucoadhesive nanoparticles of ketoconazole for bioavailability enhancement: Formulation, optimization, in vitro and ex vivo evaluation. *Drug Development and Industrial Pharmacy, 39*(4), 540–547.

Qi, L. F., Wu, L. X., Zheng, S., Wang, Y. L., Fu, H. L., & Cui, D. X. (2012). Cell-penetrating magnetic nanoparticles for highly efficient delivery and intracellular imaging of siRNA. *Biomacromolecules, 13*(9), 2723–2730.

Sogias, I. A., Williams, A. C., & Khutoryanskiy, V. V. (2008). Why is chitosan mucoadhesive? *Biomacromolecules, 9*(7), 1837–1842.

Teng, Z., Li, Y., Luo, Y., Zhang, B., & Wang, Q. (2013). Cationic β-lactoglobulin nanoparticles as a bioavailability enhancer: Protein characterization and particle formation. *Biomacromolecules, 14*(8), 2848–2856.

Teng, Z., Luo, Y. C., & Wang, Q. (2012). Nanoparticles synthesized from soy protein: Preparation, characterization, and application for nutraceutical encapsulation. *Journal of Agricultural and Food Chemistry, 60*(10), 2712–2720.

Teng, Z., Luo, Y., & Wang, Q. (2013). Carboxymethyl chitosan-soy protein complex nanoparticles for the encapsulation and controlled release of vitamin D3. *Food Chemistry, 141*(1), 524–532.

Teng, Z., Luo, Y., Wang, T., Zhang, B., & Wang, Q. (2013). Development and application of nanoparticles synthesized with folic acid conjugated soy protein. *Journal of Agricultural and Food Chemistry, 61*(10), 2556–2564.

Thongborisute, J., & Takeuchi, H. (2008). Evaluation of mucoadhesiveness of polymers by BIACORE method and mucin-particle method. *International Journal of Pharmaceutics, 354*(1–2), 204–209.

Wang, F., Yu, L., Monopoli, M. P., Sandin, P., Mahon, E., Salvati, A., et al. (2013). The biomolecular corona is retained during nanoparticle uptake and protects the cells from the damage induced by cationic nanoparticles until degraded in the lysosomes. *Nanomedicine, 9*(8), 1159–1168.

Weber, C., Coester, C., Kreuter, J., & Langer, K. (2000). Desolvation process and surface characterisation of protein nanoparticles. *International Journal of Pharmaceutics, 194*(1), 91–102.

Wiecinski, P. N., Metz, K. M., Mangham, A. N., Jacobson, K. H., Hamers, R. J., & Pedersen, J. A. (2009). Gastrointestinal biodurability of engineered nanoparticles: Development of an in vitro assay. *Nanotoxicology, 3*(3), 202–214.

Wiegand, C., Bauer, M., Hipler, U.-C., & Fischer, D. (2013). Poly(ethyleneimines) in dermal applications: Biocompatibility and antimicrobial effects. *International Journal of Pharmaceutics, 456*(1), 165–174.